J Solid State Electrochem (2009) 13:791–798
DOI 10.1007/s10008-008-0612-5

ORIGINAL PAPER

A biosensing platform based on horseradish peroxidase immobilized onto chitosan-wrapped single-walled carbon nanotubes

Huijun Jiang · Chong Du · Zhiqing Zou · Xiaowei Li · Daniel L. Akins · Hui Yang

Received: 15 April 2008 / Revised: 15 May 2008 / Accepted: 7 June 2008 / Published online: 11 July 2008

Abstract One-step, diameter-selective dispersion of single-walled carbon nanotubes (SWCNTs) has been accomplished through noncovalent complexation of the nanotubes with a water-soluble, biocompatible polymer chitosan at room temperature. Such chitosan-wrapped individual SWCNTs can be used for the immobilization of horseradish peroxidase (HRP) and be used to construct an electrode for direct bioelectrochemical sensing without an electron mediator. The direct electron transfer between HRP and the electrode surface was observed with a formal potential of approximately −0.35 V (vs. saturated calomel electrode) in phosphate buffer solution and the calculated heterogeneous electron transfer rate constant is approximately 23.5 s^{-1}. Experimental results indicate that the immobilized HRP retains its catalytic activity for the reduction of nitric oxide. Such an HRP–SWCNT–chitosan-based biosensor exhibited a rapid response time of less than 6 s and a good linear detection range for nitrite concentration, from 25 to 300 μM with a detection limit of 3 μM. The apparent Michaelis–Menten constant (K_m) and the maximum electrode sensitivity (i_{max}/K_m) are found to be 7.0 mM and 0.16 μA mM^{-1}, respectively. Both the unique electrical properties of SWCNTs and biocompatibility of chitosan enable the construction of an excellent biosensing platform for improved electrocatalysis of HRP, allowing, specifically, the detection of trace levels of nitric oxide.

Keywords Single-walled carbon nanotubes · Horseradish peroxidase · Chitosan · Direct electrochemistry · Biosensor

H. Jiang · C. Du · Z. Zou · X. Li · H. Yang (✉)
Shanghai Institute of Microsystem and Information Technology,
Chinese Academy of Sciences,
Shanghai 200050, People's Republic of China
e-mail: Hyang@mail.sim.ac.cn

H. Jiang
School of Pharmacy, Nanjing Medical University,
Nanjing 210029, People's Republic of China

D. L. Akins
CASI and Department of Chemistry,
The City College of The City University of New York,
New York, NY 10031, USA

Introduction

Although intensive interest concerning direct electron transfer between an electrode and metalloproteins in bioelectrochemistry and the related fields has been shown [1–3], the goal of formulating a biomembrane-mimicking microenvironment that facilitates electron transfer between redox proteins and enzymes and constructing a useful electrode remains an arena where much remains to be done. Research efforts in this latter regards has resulted in identification of many materials for embedding proteins that promote the direct electron transfer between redox proteins and enzymes; examples of such materials include surfactants [4], polymers [5, 6], biopolymers [7], nanoparticles [8–12], and ionic liquids [13, 14]. It is to be noted that, in particular, nanoparticles have been proved extremely useful in the preparation of nanoparticle-modified electrodes to facilitate the direct electrochemistry and bioelectrocatalysis for both enzymes and proteins. This functionality of nanoparticles is principally ascribed to the ability of such particles to provide a desirable microenvironment between the redox sites of a protein and the electrode.

Moreover, since their initial discoveries, both multiwalled and single-walled carbon nanotubes (CNTs), due to their highly unusual structural, unique electrical properties as well as a wide potential window, have been widely utilized for construction of bioelectrochemical platforms. For example,

functionalized CNTs have been coupled with hemoglobin [15], cytochrome c [16], horseradish peroxidase (HRP) [17, 18], catalase [19], microperoxidase-11 [20], glucose oxidase [21–23], glucose dehydrogenase [24], as well as other biomolecules [25] to fabricate CNT-based modified electrodes. Reviews of such applications of carbon nanotubes in electrochemistry and biosensors are provided by Gooding [26], Wang [27], and Wildgoose et al. [28]. Indeed, the useful and unique properties of CNTs have paved the way for the construction of a wide range of electrochemical biosensors exhibiting attractive analytical behaviors. Although a large number of strategies exist for modifying CNTs for use in electroanalysis and/or bioelectroanalysis applications, new strategies are needed for the vast numbers of potential applications that might serve humanity.

Here, we report new studies involving HRP, which is an important heme-containing enzyme that has been studied for more than a century. This enzyme has been extensively employed in the construction of amperometric biosensors for the detection of hydrogen peroxide, small organic peroxides and oxygen, and especially for the detection of nitric oxide (NO) [29–35]; the latter chemical was initially known as an environmental pollutant and toxin. Since the early characterization of NO as an elusive endothelial-derived relaxing factor (i.e., signaling molecule) in 1987 [36], many other physiological functions such as immune host defense, platelet aggregation, neurotransmission, vasodilation, etc. have been found to involve NO in critical steps in the biochemical processes [37, 38]. As a result, quantitative measures of NO presence in biological and environmental systems have become areas of increasing research interest. Among proposed methods for detection (including chemiluminescence, paramagnetic resonance, and spectrophotometry), electrochemical methods have shown great promise due to the simplicity, speed, and specificity of the determination [39].

Recently, we have developed a simple, efficient process for the aqueous dispersion and diameter-selective separation of single-walled carbon nanotubes (SWCNTs) with a water-soluble, environmentally friendly, biocompatible polymer chitosan (CHIT) [40]. CHIT has been extensively used as a matrix for the enzyme immobilization with attractive properties that include high permeability toward water, good adhesion, and biocompatibility [41]. SWCNTs generally existed as bundles are insoluble in essentially all the common solvents, which limit their use in biosensors due to the fact that the amount of enzymes that can be immobilized is limited, providing matrixes with sensitivities and stability properties that are not fully optimized. However, in this paper, we report that the direct electron transfer of HRP can be obtained by incorporating HRP into the chitosan-wrapped SWCNT composite films. The utilization of the chitosan-wrapped individual SWCNTs could greatly increase the contact area between the SWCNTs and enzyme; thus, it may be beneficial to an increase in sensor sensitivity and stability. This incorporation allows for the construction of an electrochemical system that evidences fast response and high sensitivity for detection of trace levels of NO, suggesting biosensor applications.

Experimental section

Materials and reagents

Purified HiPco SWCNTs were purchased from Carbon Nanotechnologies, Inc. (Houston, TX, USA) and multiwalled CNTs (MWCNTs) from Shenzhen Nanotech. Port. Co. Ltd. (Shenzhen, China). Chitosan (85% deacetylation, average molecular weight of 1×10^6 g mol^{-1}) and horseradish peroxidase (EC 1.11.1.7, RZ 3.3, 318 U mg^{-1}) were obtained from Sigma-Aldrich Corp., without further purification. Sodium nitrite was purchased from Sinopharm Chemical Reagent Co. (Shanghai, China). All other chemicals were of reagent grade and used as received.

Preparation of HRP–SWCNT–chitosan solution

A 0.5 wt.% CHIT solution was prepared by dissolving an appropriate amount of CHIT power in 0.05-mol L^{-1} HCl aqueous solution at the temperature of 80–90 °C. The resultant solution was immediately filtered and cooled, and the pH of chitosan solution was adjusted to 5.0 with concentrated NaOH; 2.5 mg of HiPco SWCNTs and 5.0 mL of 0.5 wt.% CHIT solution were then added to a vial and mixed ultrasonically in an ice bath for more than 5 h to accomplish dispersion. Subsequently, 20 mg HRP was dissolved in 2.0 mL of 0.5 mg mL^{-1} SWCNT–chitosan solution to form the HRP–SWCNT–CHIT dispersion.

Fabrication of HRP-modified electrode

Porous modified electrodes were prepared as follows. A measured volume (5 μL) of 10 mg mL^{-1} HRP–SWCNT–CHIT solution was transferred via a syringe onto a freshly polished glassy carbon (GC) disk (3 mm in diameter). After water was evaporated at room temperature, the electrode was used as the working electrode [42, 43]. The HRP–SWCNT–CHIT–GC electrode obtained was thoroughly rinsed with phosphate buffer solution and immersed into phosphate buffer solution for 60 min before use for electrochemical measurements. For comparison purposes, a HRP–MWCNT–CHIT–GC electrode was also fabricated by the method described above.

Apparatus

Raman spectra were obtained using an HR800 Jobin Horiba Raman Microscope. Samples were placed in quartz cuvettes

and excited with 514.5 nm laser radiation. All spectra were acquired in 30 s and the incident laser power (at the laser head) was approximately 10 mW. Scanning electron microscopy (SEM) was performed with an S-4700 scanning electron microscope (Hitachi, Japan) at an acceleration voltage of 10 kV.

Electrochemical measurements were performed using a CHI 730B potentiostat–galvanostat (Shanghai Chenhua Apparatus Corporation, China) and a conventional three-electrode cell. The bare GC or the modified electrode was used as the working electrode. The counter electrode was a Pt wire, and a saturated calomel electrode (SCE) was used as the reference electrode. All potentials were reported with respect to SCE. A fresh solution of $NaNO_2$ was prepared daily. The electrolyte used

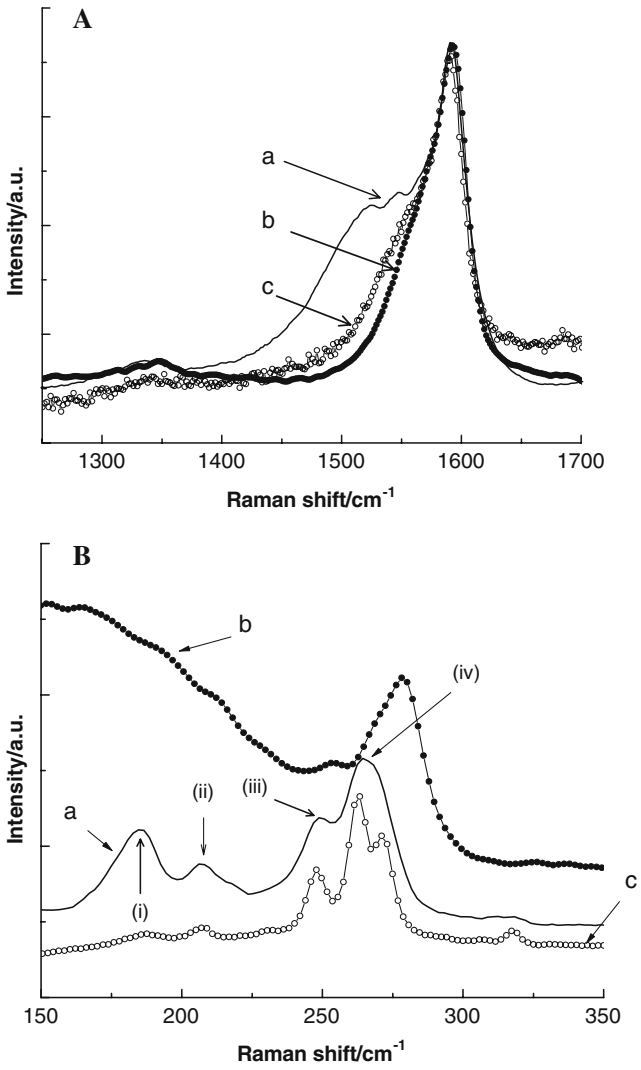

Fig. 1 **A** shows Raman spectra using a 514.5 nm excitation in the G-band region: (*a*) raw HiPco SWCNT sample, (*b*) dispersion of 0.5 mg mL^{-1} SWCNTs in chitosan solution, and (*c*) film of 0.5 mg mL^{-1} SWCNTs in chitosan solution by casting onto a GC disk. **B** shows Raman spectra in the RBM region for the same samples (*a*), (*b*), and (*c*) as above

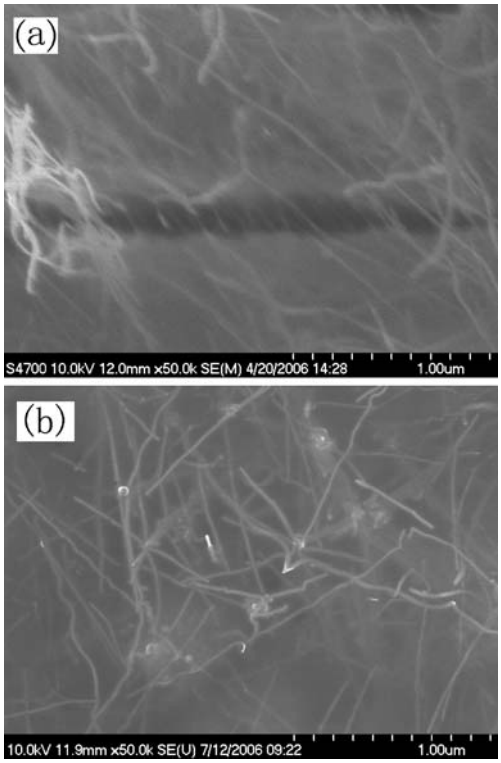

Fig. 2 SEM images of (**a**) SWCNT–CHIT film and (**b**) HRP–SWCNT–CHIT film

was 0.1 mol L^{-1} Na–phosphate buffer solutions with different pH. All the solutions were prepared with ultrapure water with a specific resistance of >18 M Ω cm^{-1}. High-purity nitrogen was used for deaeration of the solutions. During the measurements, a gentle nitrogen flow was kept above the electrolyte surface. All electrochemical experiments were performed in a thermostated cell at approximately 25 °C.

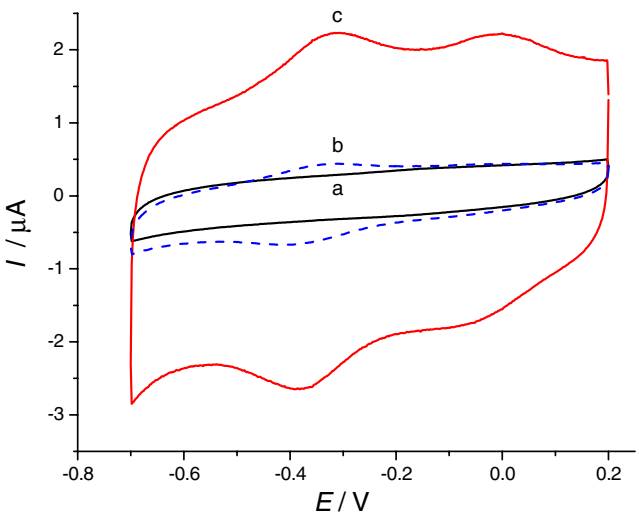

Fig. 3 CVs of (*a*) GC, (*b*) HRP–MWCNT–CHIT–GC and (*c*) HRP–SWCNT–CHIT–GC electrodes in an N_2-saturated 0.1 mol L^{-1} phosphate buffer solution (pH 6.8) at a scan rate of 0.1 V s^{-1}

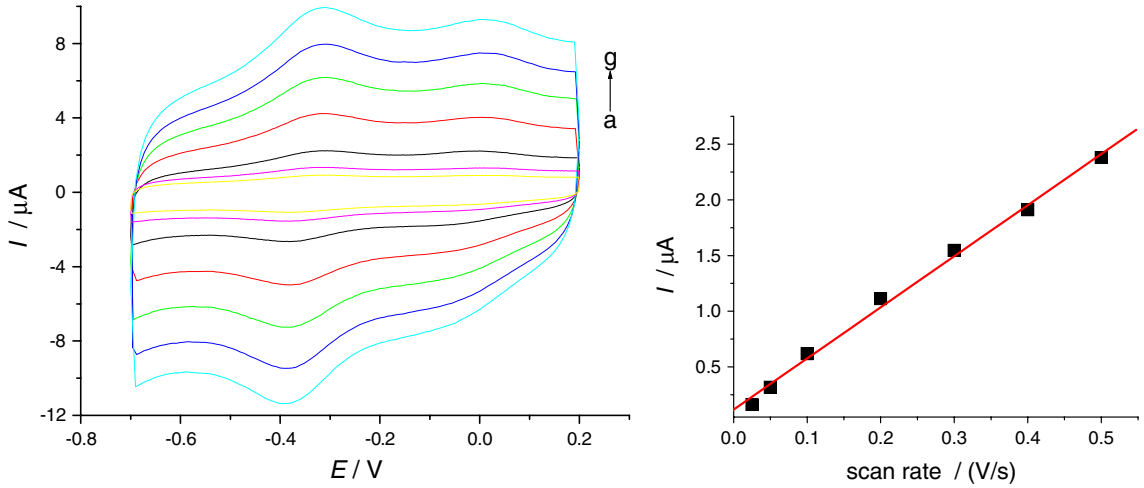

Fig. 4 CVs of HRP–SWCNT–CHIT–GC electrode in an N_2-saturated 0.1 mol L^{-1} phosphate buffer solution (pH 6.8) at scan rates of (*a*) 0.025, (*b*) 0.05, (*c*) 0.1, (*d*) 0.2, (*e*) 0.3, (*f*) 0.4, and (*g*) 0.5 V s^{-1}. *Insert* is a plot of peak current vs. scan rate

Results and discussion

Physical characterization of chitosan-wrapped single-walled carbon nanotubes films

It is to be noted that, once we dispersed SWCNTs in CHIT aqueous solution, a quantity of black powder spontaneously precipitated from dispersion (overnight), with the resultant supernatant being homogeneous, stable, and of dark color. The precipitate could not be redispersed using CHIT solution in combination with centrifugation and heating, suggesting a robust method of forming stable SWCNTs in solution.

Figure 1 shows Raman spectra using a 514.5 nm excitation in the G-band region and the radial breathing mode (RBM) region for the raw HiPco SWCNT sample, the dispersion of 0.5 mg mL^{-1} SWCNTs in CHIT solution and the film of 0.5 mg mL^{-1} SWCNTs in chitosan solution by casting onto GC disk. In Fig. 1A, curves a, b, and c, the G^+ bands located at approximately 1,590 cm^{-1} and the shoulder peaks at approximately 1,551 cm^{-1} (i.e., G^- bands) associated with the E_{2g} optical mode of graphite and characteristic of sp^2-hybridized carbon materials, indicative of the presence of SWCNTs. But the G^- bands in curves (b) and (c) have a significantly decreased intensity compared to the corresponding band of the raw HiPco sample. These findings suggest that the SWCNTs on the film keep their properties as those in solution.

In the RBM region, shown in Fig. 1B, for raw HiPco SWCNTs (curve a), there are four distinct peaks located at approximately 185, 208, 248, and 264 cm^{-1} (labeled as I, II, II, and IV, respectively), corresponding to the calculated nanotube diameters of 1.30, 1.14, 0.94, and 0.89 nm, respectively, using the equation $d(\text{nm})=223.5/\nu_{\text{RBM}}$ (cm^{-1})−12.5 as the correlation between diameter d(nm) and RBM frequency [44]. However, only two RBM bands higher than approximately 240 cm^{-1} in curves (b) and (c) are found, corresponding to the small-diameter SWCNTs. The above observations clearly indicate that smaller-diameter SWCNTs are selectively wrapped by CHIT within the SWNT–CHIT film on the surface of GC electrode.

Figure 2 shows SEM images of the SWCNT–CHIT and HRP–SWCNT–CHIT films. For the SWCNT–CHIT film, small bundled SWCNTs with a diameter range between 10 and 20 nm are observed, likely due to aggregation of SWCNTs upon drying since the SWCNTs exist in the CHIT solution as individuals. For the HRP–SWCNT–CHIT film, however, one

Table 1 Electrochemical parameters of HRP in various films

Films–electrode	pH	% Electroactive protein	$E^{\circ\prime}$ (V vs. SCE)	Average k_s (s^{-1})	Reference
HRP–SWCNT–CHIT–GC	6.8	1.2	−0.35	23.5±1.3	This work
HRP–MWCNT–CHIT–GC	6.8	0.3	−0.35	4.2±1.0	This work
HRP–HEC–PG	6.0		−0.25		[29]
HRP–SF–PE	7.0	5.2	−0.34	0.72	[30]
HRP–CS–PG	7.0	0.2	−0.33		[31]
HRP–CHIT–BMIM•BF_4–GC	7.0	1.07	−0.38		[32]
HRP–PAMAM–PG	7.0	0.8	−0.34		[33]

observes that HRP exists as small islands within the SWCNT–CHIT film. It is to be noted that, after washing by phosphate buffer solution, the images remained unchanged, suggesting good stability for the film under the conditions of their use.

Direct electrochemistry of HRP immobilized onto chitosan-wrapped single-walled carbon nanotubes

Typical cyclic voltammograms (CVs) of the bare GC and HRP-modified electrodes in an N_2-saturated phosphate-buffered saline (PBS; pH 6.8) at a scan rate of 100 mV s^{-1} are shown in Fig. 3. A comparison of curves a, b, and c, representing CVs of GC, HRP–MWCNT–CHIT–GC, and HRP–SWCNT–CHIT–GC electrodes, respectively, clearly indicates that a significantly enhanced current is observed for the HRP–SWCNT–CHIT–GC electrode. As seen in Fig. 3, curve c, a pair of weak, broad redox waves, located at approximately −0.2~0.15 V at the HRP–SWCNT–CHIT–GC electrode is attributed to the redox process of the functional oxygenated groups produced at the SWCNTs [45]. The significant enhancement of the double layer charging–discharging capacitance with SWCNTs is likely due to the high surface area and unique structural and electrical properties of individual SWCNTs wrapped by CHIT coated on the GC electrode. From curves b and c, one can observe a pair of well-defined redox peaks that appear in the potential region between −0.70 and 0.2 V, corresponding to the direct electron transfer between the heme-active site of HRP and the electrode surface. On the HRP–SWCNT–CHIT–GC electrode, the cathodic and anodic peaks are found at −0.32 and −0.38 V, respectively, indicating a peak potential separation (ΔE_p) of about 60 mV, which indicates that HRP molecules immobilized on the surface of the modified electrode undergo a 1e reversible electrochemical process. On the HRP–MWCNT–CHIT–GC

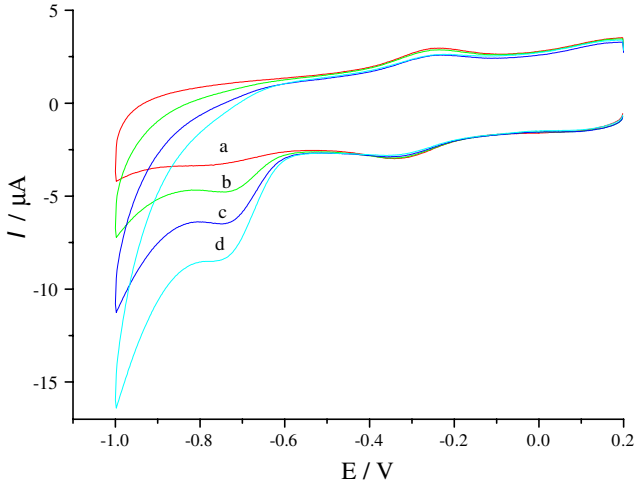

Fig. 6 CVs of HRP–SWCNT–CHIT–GC electrode in 0.1 mol L^{-1} phosphate buffer solution (pH 5.0) at scan rate of 0.1 V s^{-1} in the presence of (*a*) 0, (*b*) 0.4, (*c*) 1, and (*d*) 2 mM $NaNO_2$

electrode, the cathodic and anodic peaks are located at −0.315 and −0.398 V with the peak potential separation of approximately 83 mV, revealing that the HRP molecules immobilized on the electrode only undergo a quasireversible electrochemical process. However, as recently reported by Qian and Yang [46], no direct electron transfer between cross-linking HRP and MWCNTs–chitosan composite film was observed. The formal potential on both of our electrodes is approximately −0.35 V, which is in fairly good agreement with the heme Fe^{III}–Fe^{II} redox couples of the heme proteins [30, 33]. The peak currents in N_2-saturated PBS decreased by approximately 1% after 100 continuous cycles, suggesting a good stability of the enzyme electrode. Furthermore, it was found that the HRP immobilized into the nanocomposite film can be stored at 4 °C for several months without any

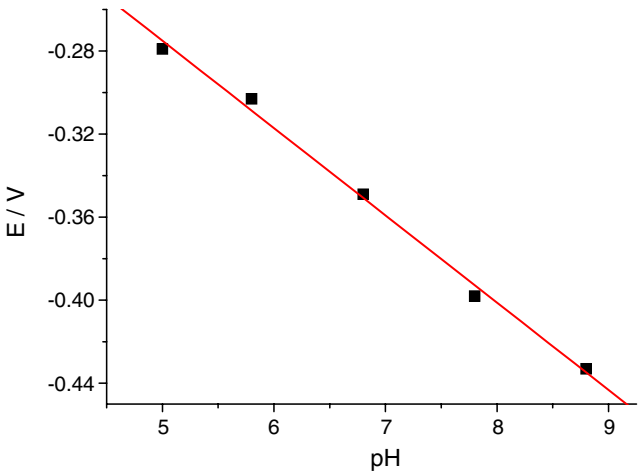

Fig. 5 Influence of pH on the redox formal potential of HRP on HRP–SWCNT–CHIT film. The data were recorded from CVs at a scan rate of 0.1 V s^{-1}

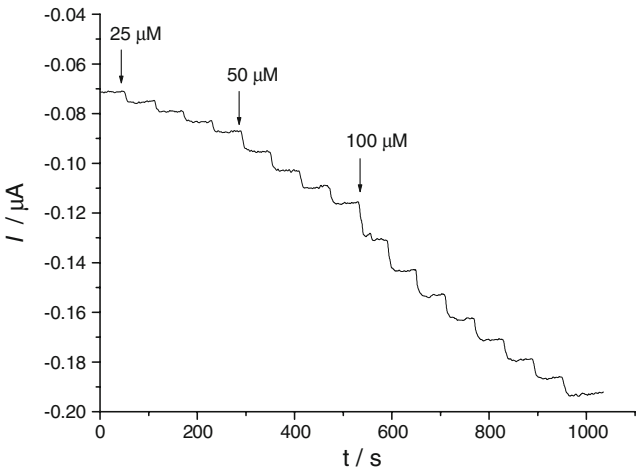

Fig. 7 Typical amperometric response of HRP–SWCNT–CHIT–GC electrode at −0.65 V on successive injection of $NaNO_2$ into 2 mL of stirring 0.1 mol L^{-1} phosphate buffer solution (pH 5.0)

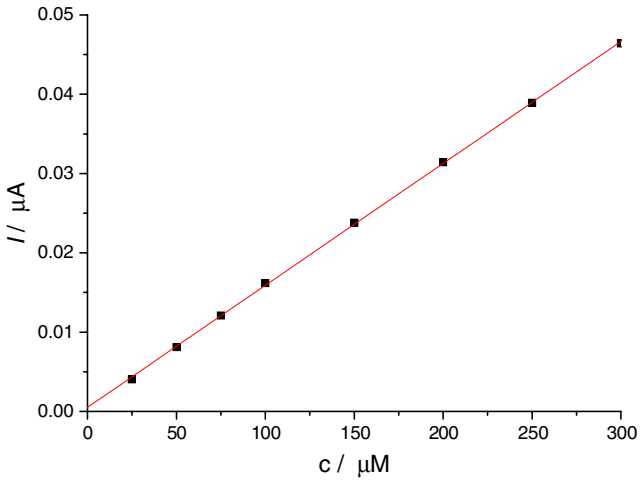

Fig. 8 Dependence of the catalytic reduction current on the concentration of $NaNO_2$

loss of the enzyme activity, again assessing a good stability of the enzyme electrode. High stability of the modified electrode could be due to the fact that the formation of network-like nanocomposite film restricts the loss of HRP.

Figure 4 shows the CVs of the HPR–SWCNT–CHIT–GC electrode in N_2-saturated PBS (pH 6.8) at various scan rates. The peak potential separation increases with scan rate ranging from 100 to 500 mV s^{-1}; however, the formal potential $(E_{pa}+E_{pc})/2$ remains essentially constant. The linear dependence of peak current on scan rate (see inset of Fig. 4) indicates that the electrochemical behavior of HRP has the typical property of a surface electrochemical process. At high scan rate (up to 5 V s^{-1} in this paper), the peak potential increases linearly with the logarithm of the scan rate. Applying the method of Laviron [47], the heterogenous electron transfer rate constant (k_s) of HRP is calculated to be approximately 23.5 s^{-1}, which is higher than the previous report [30] and higher than that on the HPR–MWCNT–CHIT–GC electrode in this paper. By the integration of the reduction wave area, the surface coverage of HRP (Γ) is calculated to be 1.95×10^{-10} mol cm^{-2}, which corresponds to about 1.2% of the total HRP amount incorporated into the film, indicating that most of the HRP molecules within the films remain inactive.

Some electrochemical parameters for the direct electron transfer of HRP immobilized on SWCNT–CHIT and MWCNT–CHIT films found in this work and those by others for other films are summarized in Table 1. Although the k_s of HRP in the SWCNT–CHIT film is only slightly larger than that in the MWCNT–CHIT film, the percentage of the electroactive HRP on the electrode surface is about three times higher, suggesting that SWCNTs are more suitable for fabrication of bioelectrochemical sensor films than are MWCNTs.

Influence of pH on HRP redox voltammetry

The influence of pH on the voltammetry of HRP–SWCNT–CHIT films was examined. Both cathodic and anodic peak potentials shifted negatively with an increase in solution pH, indicating that proton is involved in the electrode reaction of HRP. A linear relationship between the formal potential and solution pH is shown in Fig. 5. The calculated slope of $E^{\circ\prime}$ versus pH is 42 mV pH^{-1}, which is almost the same as previously reported results.[30, 33] The theoretically expected value is 59 mV pH^{-1} for the reversible transfer of a single proton and a single electron, as shown for the electrode reaction in Eq. 1 below [48].

$$\mathrm{HemeFe^{III}} + \mathrm{H^+} + e^- \rightleftharpoons \mathrm{HemeFe^{II}} \quad (1)$$

However, the value found is smaller than that predicted theoretically, which may be due to the protonation of the water molecule that is coordinated to the heme iron [30] and to the protonation of the chitosan backbone [49].

Bioelectrocatalysis of HRP immobilized on chitosan-wrapped SWCNTs

To exploit the possible applications in biosensors, the electrocatalytic reduction of nitrite at the HRP–SWCNT–CHIT–GC electrode was investigated. Figure 6 shows the CVs of the HRP–SWCNT–CHIT–GC electrode in phosphate buffer solution (pH 5.0) with the different $NaNO_2$ concentrations. A pair of reversible redox peaks at approximately −0.28 V can be assigned to the heme Fe^{III}–Fe^{II} couples. A comparison of the CVs with and without nitrite in the solution indicates that in a pH 5.0 phosphate buffer the reduction of nitric oxide starts at approximately −0.55 V and reduction peak occurs at about −0.74 V. The cathodic peak current is found to increase with the increase in $NaNO_2$ concentration, while the reduction peak of HRP(Fe^{III}) is found to decrease slightly. It is to be noted that the direct reduction of nitride at SWCNT–CHIT film was observed at the potentials more negative than −0.90 V (data not shown). Thus, the HRP–SWCNT–CHIT films decreased the overpotential of NO

Table 2 A comparison of linear range, respond time, and detection limit of the biosensors

Biosensors	Linear range (M)	Response time (s)	Detection limit (M)
HRP–SWCNT–CHIT–GC	2.5×10^{-5}~3.0×10^{-4}	6	3×10^{-6}
HRP–MWCNT–CHIT–GC	1.0×10^{-4}~1.4×10^{-3}	11	7×10^{-4}

reduction by at least 0.35 V. Our data indicate that the reduction of NO is catalyzed by HRP and that the peak at −0.74 V is due to the reduction of NO that derives from the disproportionation of nitrite [50, 51], according to the reaction shown in Eq. 2. We, furthermore, found that the NO reduction peak current decreased with increase in pH (data not shown). Also, when the pH increased to more than 6.0, the reduction peak essentially vanishes since NO cannot be produced in solutions at pH greater than 6.0, while in an acidic medium, NO is generated thermodynamically.

$$3NO_2^- + H_2O \rightleftharpoons 2NO(aq) + NO_3^- + 2OH^- \quad (2)$$

Based on the literature, the mechanisms of the electrocatalytic reduction of NO at HRP–SWCNT–CHIT films is suggested to be the following [52]:

$$HRPFe(III) + e \rightarrow HRPFe(II) \quad (3)$$

$$HRPFe(II) + NO \rightarrow HRPFe(II) - NO \quad (4)$$

$$2\,HRPFe(II) - NO + 2\,e + 2\,H^+ \rightarrow 2\,HRPFe(II) + H_2O + N_2O \quad (5)$$

To evaluate the application of the HRP–SWCNT–CHIT film for the detection of nitric oxide, the current was monitored when aliquots of $NaNO_2$ were injected into pH 5.0 phosphate buffer solution every 60 s at a given potential of −0.65 V; Fig. 7 shows the current response to the addition of $NaNO_2$. The electrocatalytic current increases with successive addition of $NaNO_2$. The relationship between catalytic reduction current and $NaNO_2$ concentration is shown in Fig. 8. From Figs. 7 and 8, it can be found that the maximum time required to reach a steady-state current occurred within 6 s and that the response was linear for the concentration range 25 to 300 μM, with a correlation coefficient of 0.9999. The detection limit of the electrode was found to be 3 μM, based on the signal-to-noise ratio of 3. The apparent Michaelis–Menten constant (K_m) and the maximum electrode sensitivity (i_{max}/K_m) are found to be 7.0 mM and 0.16 μA mM^{-1}, respectively. For comparison, electrochemical detection of nitric oxide on the HRP–MWCNT–CHIT film was also evaluated. The results obtained together with those obtained on the HRP–SWCNT–CHIT film are summarized in Table 2. These parameters are comparable to or improvements in measurements reported by others for the determination of nitric oxide [31, 34, 38]. One also can clearly deduce that the HRP–SWCNT–CHIT electrode can be used for the determination of trace levels of NO due to its rapid response time, good detection limit, and linear response range.

Conclusions

Single-walled carbon nanotubes wrapped by a water-soluble, environmentally friendly, biocompatible polymer chitosan were employed for the construction of a bioelectrochemical platform. The immobilization of HRP within the chitosan-wrapped SWNT film is shown to be a highly efficient method for the development of a new class of very sensitive, stable, and reproducible biosensors. Horseradish peroxidase incorporated into the SWCNT–CHIT films can successfully accelerate the direct electron transfer between HRP and the electrode with a formal potential of about −0.35 V in phosphate buffer solution and a heterogenous electron transfer rate constant of about 23.5 s^{-1}. Moreover, the immobilized HRP is found to retain its catalytic activity toward the reduction of nitric oxide. Such an HRP–SWCNTs–chitosan-based biosensor exhibited a high sensitivity, a rapid response time, and a good linear range from 25 to 300 μM with a detection limit of 3 μM for the nitrite detection. Both the unique electrical properties of SWCNTs and the biocompatibility of chitosan enable us to construct an excellent biosensing platform, which may supply an application perspective as a new type of NO biosensor.

Acknowledgements We would like to thank the National Natural Science Foundation of China (20673136, 20706056), the National "863" High-Technology Research Program of China (2006AA05Z136, 2007AA05Z141), the 100 People Plan Program of Chinese Academy of Sciences, and the Pujiang Program of Shanghai City (No. 06PJ14110) for support of this work.

References

1. Taniguchi I (1993) In: Schultz FA, Taniguchi I (eds) Redox mechanisms and interfacial properties of molecules of biological importance. Pennington, New Jersey, p 9
2. Hawkridge FM, Taniguchi I (1995) Comments Inorg Chem 17:163
3. Armstrong FA (1990) In: Clarke MJ, Goodenough JB, Ibers JA, Jorgensen CK et al (eds) Structure and bonding. vol. 72. Springer, Berlin, p 137
4. Liu XJ, Xu Y, Ma X, Li G (2005) Sensors and Actuators B 106:284
5. Senaratne W, Andruzzi L, Ober CK (2005) Biomacromolecules 6:2427
6. McQuade DT, Pullen AE, Swager TM (2000) Chem Rev 100:2537
7. Krajewska B (2004) Enzyme and Microbial Technology 35:126
8. Curulli A, Valentini F, Padeletti G, Cusma A, Ingo GM, Kaciulis S, Caschera D, Palleschi G (2005) Sensors and Actuators B 111:526
9. Merkoci A, Aldavert M, Marin S, Alegret S (2005) Trends in Analytical Chemistry 24:341
10. Arben M, Martin P, Xavier L, Briza P, Manel V, Salvador A (2005) Trends in Analytical Chemistry 24:826
11. Gooding JJ (2005) Electrochimica Acta 50:3049
12. Murphy L (2006) Current Opinion in Chemical Biology 10:177
13. Zhao F, Wu X, Wang MK, Liu Y, Gao L, Dong SJ (2004) Anal Chem 76:4960
14. DiCarlo CM, Compton DL, Evans KO, Laszlo JA (2005) Bioelectrochemistry 68:134

15. Cheng WX, Jin GY, Zhang YZ (2006) Sensors and Actuators B 114:40
16. Wang JX, Li MX, Shi ZJ, Li NQ, Gu ZN (2002) Anal Chem 74:1993
17. Zhang YJ, Li J, Shen YF, Wang MJ, Li JH (2004) J Phys Chem B 108:15343
18. Yu X, Chattopadhyay D, Galaska I, Papadimitrakopoulous F, Rusling JF (2003) Electrochem Commun 5:408
19. Wang L, Wang JX, Zhou FM (2004) Electroanalysis 16:627
20. Gooding JJ, Wibowo R, Liu JQ, Yang WR, Losic D, Orbons S, Mearns FJ, Shapter JG, Hibbert DB (2003) J Am Chem Soc 125:9006
21. Azamian BR, Davis JJ, Coleman KS, Bagshaw CB, Green MLH (2002) J Am Chem Soc 124:12664
22. Patolsky F, Weizmann Y, Willner I (2004) Angew Chem Inter Ed 43:2113
23. Wang J, Musameh M (2005) Anal Chim Acta 539:209
24. Zhang MG, Smith A, Gorski W (2004) Anal Chem 76:5045
25. Hrapovic S, Liu Y, Male KB, Luong JHT (2004) Anal Chem 76:1083
26. Gooding JJ (2005) Electrochim Acta 50:3049
27. Wang J (2005) Electroanalysis 17:7
28. Wildgoose GG, Banks CE, Leventis HC, Compton RG (2006) Microchim Acta 152:187
29. Azevedo AM, Martins VC, Prazeres DMF, Vojinovic V, Cabral JMS, Fonseca LP (2003) Biotechnology Annual Review 9:199
30. Liu XJ, Chen T, Liu LF, Li GX (2006) Sensors and Actuators B 113:106
31. Wu YH, Shen QC, Hu SS (2006) Anal Chim Acta 558:179
32. Huang H, Hu NF, Zeng YH, Zhou G (2002) Anal Biochem 308:141
33. Lu XB, Zhang Q, Zhang L, Li JH (2006) Electrochem Commun 8:874
34. Shen L, Hu NF (2004) Biochimica et Biophysica Acta 1608:23
35. Chattopadhyay K, Mazumdar S (2000) Bioelectrochemistry 53:17
36. Ignarro LJ, Bugga GM, Wood KS, Byrns RE, Chaudhuri G (1987) Proc Natl Acad Sci USA 84:9265
37. Toda N, Okamura T (2003) Pharmacol Rev 55:271
38. Miranda KM (2005) Coord Chem Rev 249:433
39. Liu XJ, Zhang WJ, Huang YX, Li GX (2004) J Biotech 108:145
40. Yang H, Wang SC, Mercier P, Akins DL (2006) Chem Commun 1425
41. Sorlier P, Denuziere A, Viton C, Domard A (2001) Biomacromolecules 2:765
42. Tsai YC, Li SC, Chen JM (2005) Langmuir 21:3653
43. Zhao F, Wu XE, Wang MK, Liu Y, Gao LX, Dong SJ (2004) Anal Chem 76:4960
44. Bachilo SM, Strano MS, Kittrell C, Hauge RH, Smalley RE, Weisman RB (2002) Science 298:2361
45. Gong KP, Yan YM, Zhang MN, Su L, Xiong SX, Mao LQ (2005) Anal Sci 21:1383
46. Qian L, Yang XR (2006) Talanta 68:721
47. Laviron E (1979) J Electroanal Chem 101:19
48. Bond AM (1980) Modern polarographic methods in analytical chemistry. Marcel Dekker, New York, p 27
49. Yi H, Wu LQ, Bentley WE, Ghodssi R, Rubloff GW, Culver JN, Payne GF (2005) Biomacromolecules 6:2881
50. Pan KC, Chuang CS, Cheng SH, Su YO (2001) J Electroanal Chem 501:160
51. Stanbury DM, DeMame MM, Doodloe G (1989) J Am Chem Soc 111:5496
52. Bayachou M, Lin R, Cho W, Farmer PJ (1998) J Am Chem Soc 120:9888